

Interplay of antiferromagnetism, ferromagnetism and superconductivity in $\text{EuFe}_2(\text{As}_{1-x}\text{P}_x)_2$ single crystals

H. S. Jeevan,¹ Deepa Kasinathan,² H. Rosner,² and P. Gegenwart¹

¹*I. Physikalisches Institut, Georg-August-Universität Göttingen, D-37077 Göttingen, Germany and*

²*Max-Planck-Institut für Chemische Physik fester Stoffe, 01187 Dresden, Germany*

We report a systematic study on the influence of antiferromagnetic and ferromagnetic phases of Eu^{2+} moments on the superconducting phase upon doping the As site by isovalent P, which acts as chemical pressure on EuFe_2As_2 . Bulk superconductivity with transition temperatures of 22 K and 28 K are observed for $x=0.16$ and 0.20 samples respectively. The Eu ions order antiferromagnetically for $x \leq 0.13$, while a crossover is observed for $x \geq 0.22$ whereupon the Eu ions order ferromagnetically. Density functional theory based calculations reproduce the observed experimental findings consistently. We discuss in detail the coexistence of superconductivity and magnetism in a tiny region of the phase space and comment on the competition of ferromagnetism and superconductivity in the title compound.

PACS numbers: 71.20.Eh, 75.10Dg, 75.20.Hr

The appearance of superconductivity (SC) in the vicinity of a magnetic instability is often related to quantum critical phenomena,^{1,2} although only in few cases the magnetic excitations which mediate the SC pairing have been identified.³ The discovery of superconductivity upon suppression of magnetism in iron containing pnictides and chalcogenides has created great interest in the field of condensed matter physics. Among the various members of the iron containing pnictides, there are three main families of materials, which show SC transitions upon substitution by a dopant or upon applying external pressure. They are, (i) the quaternary ‘1111’ compounds, $R\text{FeAsO}$, where R represents a lanthanide such as La, Ce, Sm etc.⁴⁻⁷ with transition temperatures as high as 56 K; (ii) the ternary $A\text{Fe}_2\text{As}_2$ ($A = \text{Ca}, \text{Sr}, \text{Ba}, \text{Eu}$)⁸⁻¹¹ systems, also known as ‘122’ systems that exhibit superconductivity up to 38 K; and (iii) the binary chalcogenide ‘11’ systems (*eg.* FeSe) with superconducting transition temperatures up to 14 K.¹² In this work we concentrate on EuFe_2As_2 , a special member of the 122 family. EuFe_2As_2 exhibits a spin density wave (SDW) in the Fe sublattice together with a structural transition at 190 K and in addition an antiferromagnetic (AF) order at 19 K due to Eu^{2+} ions.¹³ Superconductivity can be achieved in this system by substituting Eu with K or Na (Ref. 9 and 14), As with P (Ref. 15) and upon application of external pressure.¹⁶

Isovalent P doping on the As site in EuFe_2As_2 without introducing holes or electrons, simulates a scenario generally referred to as “chemical pressure”. While the Eu^{2+} moments order antiferromagnetically (A-type) at 19 K in the parent compound, ferromagnetic order at 27 K is found for the end member EuFe_2P_2 .¹⁷ In early 2009, Ren and coworkers¹⁵ reported on the co-existence of superconductivity and ferromagnetism (FM) of the Eu^{2+} moments in polycrystalline samples of $\text{EuFe}_2(\text{As}_{0.7}\text{P}_{0.3})_2$. On the other hand systematic studies by the same group on Ni doping in $\text{EuFe}_{2-x}\text{Ni}_x\text{As}_2$ showed only FM ordering of the Eu^{2+} moments but no superconductivity.¹⁹ In contrast, superconductivity has been reported upon Ni doping of the Fe site for the other

three members of the $A\text{Fe}_{2-x}\text{Ni}_x\text{As}_2$ ($A = \text{Ca}, \text{Sr}, \text{Ba}$) family.²²⁻²⁴ Based on these reports, the physical properties of both Ni and P doped EuFe_2As_2 samples seem to contradict each other in terms of competition or coexistence of FM and SC phases. In this paper, we report on the detailed investigation of the resistivity, magnetization and specific heat measurements using well-characterized single crystals of $\text{EuFe}_2(\text{As}_{1-x}\text{P}_x)_2$ and show the presence of bulk superconductivity up to 28 K. Our measurements also prove that in this system, the FM (Eu^{2+} ions) and SC phases compete with each other, rather than coexist, in contradiction to the claim of Ref. 15. Bulk SC coexisting with AF Eu^{2+} ordering is only found in a very narrow regime of P doping, where the Fe SDW transition has just been suppressed. The systematic study of P doping on single crystals allows us to draw a phase diagram that is complex and rich with five different phases.

A series of single crystals of $\text{EuFe}_2(\text{As}_{1-x}\text{P}_x)_2$ with a range of P doping were synthesized using the Bridgman method. Stoichiometric amounts of starting elements (Eu 99.99%, Fe 99.99%, As 99.99999% and P 99.99%) were taken in an Al_2O_3 crucible, which was then sealed in a Ta-crucible under Argon atmosphere. The sealed crucible was heated at a rate of 50°C/hour up to 1300°C, kept for 12 hours at the same temperature and then cooled to 950°C with a cooling rate of 3°C/hour. We obtained large plate-like single crystals using this process with dimensions of 5 x 3 mm² in the ab -plane. In addition to the plate-like single crystals, we also found a secondary polycrystalline phase which was identified as Fe_2P . All the elements and sample handling were carried out inside a glove box filled with Ar atmosphere. The quality of the single crystals was checked using the Laue method and powder x-ray diffraction and additionally with scanning electron microscopy equipped with energy dispersive x-ray analysis (EDX). Electrical resistivity and specific heat were measured using a Physical Properties Measurement System (PPMS, Quantum Design, USA). Magnetic properties were measured using Superconducting Quantum Interference Device (SQUID) magnetome-

TABLE I. Tetragonal lattice parameters (300 K) of $\text{EuFe}_2(\text{As}_{1-x}\text{P}_x)_2$ crystallizing in the ThCr_2Si_2 -type structure as a function of phosphorus substitution (x), which is determined by EDX

x	a (Å)	c (Å)
0	3.907	12.114
0.15	3.891	11.948
0.16	3.890	11.930
0.20	3.887	11.890
0.22	3.889	11.877
0.26	3.889	11.870
0.38	3.885	11.774
1	3.816	11.248

ter procured from Quantum Design. The change of the electronic properties with phosphorus doping has been investigated by angle-resolved photoemission spectroscopy (ARPES) and optical conductivity measurements^{25–27} on our single crystals. A non-rigid-band like change of the electronic structure was found, different to the case of electron or hole doping. The Eu^{2+} moments have negligible influence on the electronic structure of the valence band. In this paper we focus on the interplay of Eu^{2+} magnetism on the formation of SC.

The powder diffraction pattern of all the samples can be indexed using the tetragonal ThCr_2Si_2 structure type. The variation of the lattice parameters with respect to P content is collected in Table. I, wherein the actual P content is given as determined by EDX. Similar to other isovalent substitutions of 122 systems discussed in literature¹⁸, phosphorus substitution on the As site leads to a dramatic decrease of FeAs-layer thickness, which indicates that P doping mainly affects the c lattice parameter. We also observe that the decrease along the tetragonal axis (c lattice parameter) is more pronounced compared to the changes in the ab plane (*cf.* Table. I).

The temperature dependence of the normalized resistivity (with the current measured in the basal ab -plane) is shown in Fig. 1 for the single crystals of $\text{EuFe}_2(\text{As}_{1-x}\text{P}_x)_2$. The sample quality was determined by the residual resistivity ratio (RRR) value, $\rho_{300\text{K}}/\rho_0$, where ρ_0 is the residual resistivity at 2K and $\rho_{300\text{K}}$ is the resistivity at room temperature. The temperature dependence of the resistivity shows a metallic behavior for the entire doping range. For the parent compound EuFe_2As_2 , we observe both the SDW anomaly associated with the structural and magnetic transition of the Fe sublattice¹³ at 190K (T_{SDW}) and the anomaly at 19K (T_N) associated with the AF ordering of the Eu^{2+} moments. Upon doping with P, for the lowest P content studied here $x=0.12$, the resistivity decreases linearly with temperature down to 90 K, whereupon we observe an anomaly which is likely due to the SDW transition. No further anomalies are observed for this sample. When the P content is increased, the SDW transition is

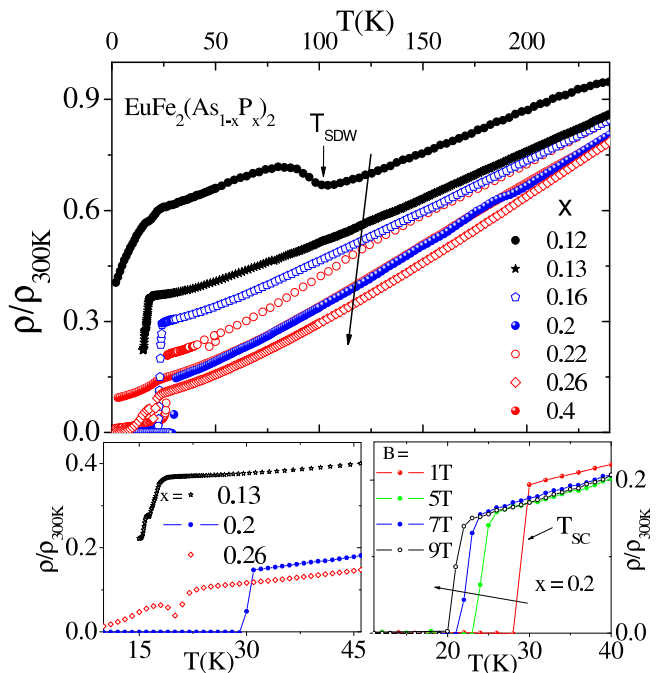


FIG. 1. (Color online) Temperature dependence of the in-plane (ab -plane) resistivity for various $\text{EuFe}_2(\text{As}_{1-x}\text{P}_x)_2$ single crystals. The data are normalized to the room temperature resistivity. Lower left panel: Low temperature part of the normalized in-plane resistivity for selected samples. Lower right panel: Normalized in-plane resistivity of the superconducting sample ($x=0.2$) for various values of applied magnetic field.

fully suppressed and a sudden drop in the resistivity indicative of a superconducting (SC) transition is observed for $x=0.16$ at 22 K and for $x=0.2$ at 29 K. For $x=0.22$, a sharp drop in the resistivity is observed around 25 K but the normalized resistivity does not go to zero. For larger P concentrations, $x \geq 0.26$, the SC transition is fully suppressed. The lower right panel of Fig. 1 shows the field dependence of the normalized resistivity of the SC transition temperature for the $x=0.2$ sample. The $\rho(T)/\rho_{300\text{K}}$ shows a sharp drop below 30 K in zero magnetic field and shifts to lower temperatures as the field increases and reaches 22 K at 9 T.

We measured the dc magnetic susceptibility for selected compositions to obtain more insights regarding the nature of the magnetic and SC phases, with the applied magnetic field parallel to the ab plane. Fig. 2 shows the field cooled (FC) and zero field cooled (ZFC) susceptibility at 50 Oe, for $x = 0.13, 0.16$ and 0.26 . For the underdoped sample ($x=0.13$) both ZFC and FC data show only the anomaly at 17 K due to AF ordering of the Eu^{2+} moments. There are no signs for a SC phase for this sample, consistent with the resistivity measurements. For the optimally doped $x=0.16$ sample, the susceptibility shows a pronounced diamagnetic step at 22 K, evidence for a bulk SC transition, consistent with the sharp drop observed in resistivity below 22 K. Further increasing the P content to $x=0.26$, the magnetic susceptibility shows only

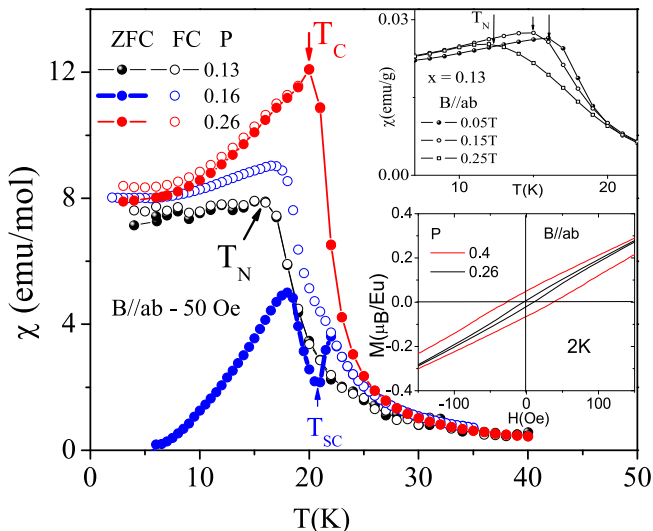


FIG. 2. (Color online) Temperature dependence of the magnetic susceptibility for $\text{EuFe}_2(\text{As}_{1-x}\text{P}_x)_2$. Upper inset: Field dependence of the AF transition for the $x=0.13$ sample. Lower inset: Isothermal magnetization at 2K of $x=0.26$ and 0.4 samples which show a FM ordering of the Eu^{2+} moments.

an anomaly at 20K due to the FM ordering of the Eu^{2+} moments (discussed later). It is clear from the magnetic susceptibility measurements, that bulk SC phase transition is observed only for the $x=0.16$ sample, while no sign for a SC phase is inferred for $x=0.13$ and 0.26 samples. The inset of Fig. 2 shows the field dependence of T_N for the under-doped sample, $x=0.13$. With increasing fields, T_N is shifted to lower values. This is indicative of the AF ordering of the Eu^{2+} moments. Upon increasing the P content to $x=0.26$, the Eu ordering changes from AF to FM. The FM ordering of the $x=0.26$ and 0.4 samples are confirmed by isothermal magnetization measurements at 2K shown in the lower inset of Fig. 2. A small but clear hysteresis loop is observed as a function of applied field, which is consistent with similar observation in the ferromagnetically ($T_C=29\text{K}$) ordered end member EuFe_2P_2 .¹⁷ Previously, Ren and co-workers¹⁵ claimed the coexistence of SC with FM for a $x=0.3$ polycrystal, which displays a tiny (10^{-2} emu/mol) diamagnetic contribution to the susceptibility together with a broadened resistive transition at 25K and which also shows a re-entrance behavior around 16K. The data on single crystals presented here indicate clear bulk SC only within the concentration range $0.16 \leq x \leq 0.2$. At large P doping, where Eu displays FM ordering, SC appears to be suppressed.

Another confirmation for the bulk nature of the magnetic and SC phases is obtained by measuring the specific heat (C_p) in the temperature range from 35K down to 2K. The data is collected in Fig. 3 for an under-doped ($x=0.13$), optimally doped ($x=0.2$) and over-doped ($x=0.4$) single crystals. The plot shows clear anomalies for both AF (T_N) and FM (T_C) phase transitions for $x=0.13$ and 0.4 respectively. Due to strong

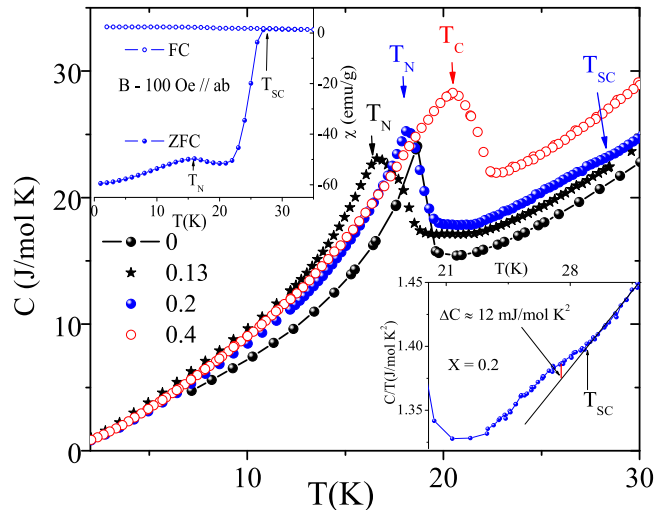


FIG. 3. (Color online) Evaluation of AF (T_N) and FM (T_C) ordering temperatures as a function of phosphorus substitution in the specific heat. Lower inset shows the anomaly of the SC phase transition for the $x=0.2$ sample. Upper inset shows the dc-magnetic susceptibility for ZFC and FC experiments in applied field of 50 Oe for the $x=0.2$ sample.

contributions at low temperatures from the phonons and Eu^{2+} magnetic moments to the specific heat, it is hard to observe an anomaly at the SC phase transition, however a small anomaly (lower inset of Fig. 3) in the raw data (without subtracting any phonon contribution) is resolved below 28K for $x=0.2$. This observation is consistent with the diamagnetic step observed in the magnetic susceptibility (upper inset of Fig. 3) as well as the drop in resistivity (Fig. 1). In addition, the magnetic susceptibility for $x=0.2$ (ZFC at 50 Oe) shows a small anomaly at 20K corresponding to the AF transition of the Eu^{2+} moments, indicative of a co-existence of AF and SC for this sample. Based on these thermodynamic measurements, we infer that both the magnetism and SC are of bulk nature and furthermore only AF and SC phases co-exist for $\text{EuFe}_2(\text{As}_{1-x}\text{P}_x)_2$. A single crystal with $x=0.18$, displaying a SC transition at 28K has also been studied by optical conductivity measurements²⁷ above and below T_C . A BCS fit revealed a s-wave type gap with $2\Delta = 3.8k_B T_C$.

The results obtained from the different measurements allow us to draw the electronic phase diagram of $\text{EuFe}_2(\text{As}_{1-x}\text{P}_x)_2$ as a function of phosphorus doping. The transition temperatures were determined from specific heat, resistivity and magnetic susceptibility measurements. Fig. 4 shows a complex phase diagram, wherein we have identified five different phases. The parent compound EuFe_2As_2 with tetragonal symmetry is paramagnetic at high temperatures (above 190K), while below 190K, the structure changes to orthorhombic and the Fe moments order antiferromagnetically (SDW). In addition, below 19K, the system undergoes another AF transition associated with the Eu^{2+} moments. Upon isovalent doping of the As site with P in $\text{EuFe}_2(\text{As}_{1-x}\text{P}_x)_2$,

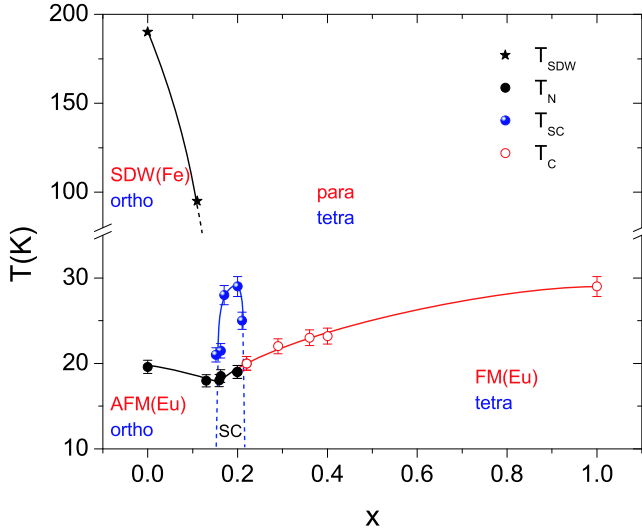


FIG. 4. (Color online) The complex phase diagram for $\text{EuFe}_2(\text{As}_{1-x}\text{P}_x)_2$ as a function of P. The solid lines act as a guide to the eye and the dotted lines are extrapolation using the available experimental data to close the superconducting dome.

for $0.16 \leq x \leq 0.22$ we observe bulk SC phase transitions coexisting with AF ordering of the Eu^{2+} moments. Further increasing the P content, $x \geq 0.26$, SC is completely suppressed and the Eu^{2+} sublattice magnetic interaction changes from AFM to FM. Recently, Nandi *et al.* proposed²⁰ that the coupling between orthorhombicity and superconductivity is indirect and claim that it arises due to the strong competition between magnetism (of Fe) and superconductivity in Co doped BaFe_2As_2 systems. This means that the orthorhombic to tetragonal transition occurs at temperatures above the onset of Fe magnetic (SDW) order and the orthorhombic structure could continue to exist in the superconducting phase too. Similar arguments can be used for the current phase diagram of $\text{EuFe}_2(\text{As}_{1-x}\text{P}_x)_2$ where most likely AF (Eu) and SC phase coexist with the orthorhombic phase. The FM phase is not favorable for SC with either s- wave or d- wave theories, because the Zeeman effect arising due to ferromagnetism will transfer the singlet into a triplet which will eventually lead to the breakdown of the Cooper pairs. Hence we believe that the report of Ren and co-workers¹⁵ on the coexistence of SC and ferromagnetism in $\text{EuFe}_2(\text{As}_{0.7}\text{P}_{0.3})_2$ is likely a misinterpretation of data obtained on polycrystalline samples, which might have inhomogeneous phosphorus doping concentration. In general, single crystals are compositionally more homogeneous than polycrystalline samples, and if there was even a 1% volume fraction of the superconducting phase, one should observe a drop (not zero) in the resistivity measurements. In our single crystals, with $x=0.38$, we did not observe any such drop in resistivity. At this juncture, we would also like to note that, by crushing a single crystal of $\text{EuFe}_2(\text{As}_{0.62}\text{P}_{0.38})_2$ into a powder we repeated all our measurements and did not

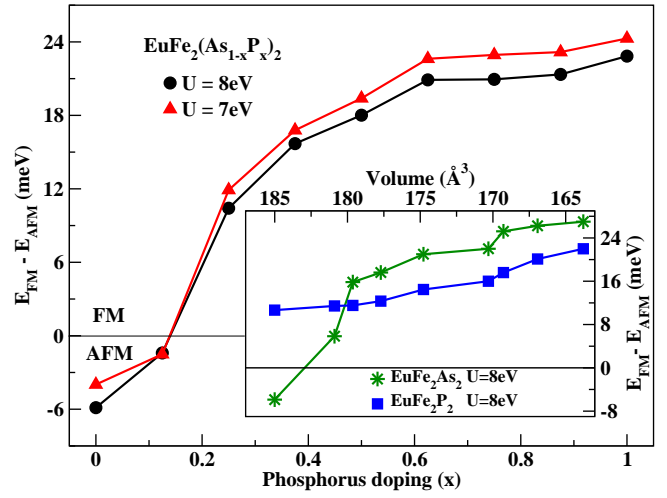


FIG. 5. Energy difference between FM and AF aligned Eu^{2+} moments along the c -axis, as a function of Phosphorus content in $\text{EuFe}_2(\text{As}_{1-x}\text{P}_x)_2$. Along the y -axis, the ground state is AFM below zero and FM above zero. Inset: Energy difference (same as main panel) as a function of reduced volume for the two end-members EuFe_2As_2 and EuFe_2P_2 . The data points in the inset and the main panel have a one-to-one correspondence.

notice any change in our descriptions (*i.e.* only FM ordering of the Eu^{2+} moments was observed, but no SC phase transition).

For a microscopic understanding of the inter-layer coupling of the Eu^{2+} moments in $\text{EuFe}_2(\text{As}_{1-x}\text{P}_x)_2$, we have carried out total energy calculations using the full-potential local orbital code (FPLO).²⁸ We used the Perdew-Wang²⁹ flavor of the exchange-correlation potential and the energies were converged on a dense k -mesh consisting of 20^3 points. The localized Eu $4f$ states were treated on a mean-field level by using the LSDA+ U (local-spin-density-approximation + strong correlations) approach, applying the so called “atomic limit” (AL) double-counting scheme.³⁰ In general, the physically relevant value of the strong correlations of the Eu^{2+} ion are inferred from various spectroscopy techniques, especially by photoemission spectroscopy (PES) experiments. Owing to the lack of such experiments for EuFe_2As_2 , we have therefore used a U value of 7-8 eV. The robustness of our results and consequently the interpretations were checked for consistency with varying U values. The Fe $3d$ states were treated on an itinerant level (LSDA) without additional correlations. The partial P substitution was modeled by the construction of supercells of various sizes. The randomness in possible substitution positions were taken into account, by allowing phosphorus to occupy different possible combinations of the four-fold $4e$ As sites. The lattice parameters for the various supercells were obtained by interpolating the experimental data reported in Table I. The As/P z -position was kept fixed at 0.362 throughout. Based on density functional theory based calculations, previously¹³ we have shown that the

Eu and Fe sublattices are quite de-coupled in EuFe_2As_2 . This result is also corroborated experimentally by showing that the Eu^{2+} moments only play a minor role in the electronic transport properties.³¹ Presently, our goal is to obtain an estimate for the Eu inter-layer coupling below T_N or T_C , while the Fe sublattice is retained in the SDW pattern. The results from our calculations are collected in Fig. 5. For $x < 0.2$, the ground state of $\text{EuFe}_2(\text{As}_{1-x}\text{P}_x)_2$ is AF, consistent with the above mentioned experimental results. The energy difference between the AF (ground state) and FM alignment of the Eu^{2+} moments is quite small (0 to 6 meV per formula unit). This implies a rather weak inter-layer coupling for the Eu sublattice. Any small external effects (impurities, doping, etc.) can easily flip the Eu spins from AF to FM. This has also been shown experimentally by Xiao and co-workers³² for the parent compound EuFe_2As_2 , wherein below T_N they observe a field-induced spin reorientations to the FM state for an applied field of just 1 T in the ab -plane and at 2 T along the c -axis. For $x > 0.2$, FM inter-layer coupling between the Eu^{2+} moments becomes favorable (*i.e.* ground state is FM) and continues to remain so for larger P substitutions, consistent with the present experimental observations. The Fe sublattice remains magnetic for $0 \leq x \leq 0.875$ with a slight reduction of the individual magnetic moments with increasing phosphorus content. The Fe sublattice becomes non-magnetic for the end member of this substitution series EuFe_2P_2 , while the rare-earth Eu remains divalent in the entire substitution range. These results are also consistent with the recently reported experimental findings of Feng and co-workers¹⁷ for EuFe_2P_2 . Another recent report by Sun and collaborators³⁴ witness a valence change of europium from a 2+ to a 3+ state in $\text{EuFe}_2\text{As}_{1.4}\text{P}_{0.6}$ at ambient conditions. This valence change behavior seems rather counterintuitive, since the end member EuFe_2P_2 is a well known ferromagnet with divalent europium.³³ Nevertheless, we investigated the possibility of such a valence change in our calculations and found that europium favors the divalent state in the entire substitution range.

As mentioned earlier, without the introduction of additional holes or electrons, isovalent doping of As by P simulates chemical pressure in $\text{EuFe}_2(\text{As}_{1-x}\text{P}_x)_2$. Since the size of phosphorus ion is smaller than arsenic ion, the lattice parameters shrink with increasing phosphorus content (refer Table. I). The substitution of As by P and as well as the decrease in the volume of the unit cell together influence the magnetism of the Eu sublattice. In order to de-couple these two effects; substitution and volume reduction and henceforth obtain a deeper under-

standing of the chemistry and lattice effects respectively, we performed two further calculations: (i) parent compound EuFe_2As_2 as a function of reduced volume; and (ii) end member EuFe_2P_2 as a function of reduced volume. The former calculations provide information on the lattice effects, while the latter calculations explain the effects of substitution. Our findings are summarized in the inset of Fig. 5. The data points in the inset have a one-to-one correspondence with the doping (x) values in the main panel. The ground state of EuFe_2As_2 changes from AF to FM earlier than that of $\text{EuFe}_2(\text{As}_{1-x}\text{P}_x)_2$. The As $4p$ states are more extended than P $3p$ states, which when combined with a strong decrease of the c -axis tends to influence the inter-layer magnetic interaction of the Eu^{2+} ions more than phosphorus. On the contrary, Eu^{2+} moments in EuFe_2P_2 remains FM for all volumes in our calculations. The reported ambient conditions volume from experiments for EuFe_2P_2 is 163.79 \AA^3 (Ref. 17) with FM aligned Eu ions. Expanding this lattice to 185 \AA^3 (room-temperature volume of EuFe_2As_2) reduces the strength of the FM interaction between the inter-layer Eu ions, but does not flip the spins. Combining these results, we infer that the lattice effects play a major role in influencing the interplay of Eu-magnetism in $\text{EuFe}_2(\text{As}_{1-x}\text{P}_x)_2$.

In summary, we have systematically grown good quality single crystals and studied the transport, magnetic and thermodynamic properties on a series of $\text{EuFe}_2(\text{As}_{1-x}\text{P}_x)_2$ samples and explore the details of the interplay of AF and FM phase of Eu^{2+} moments with the SC phase as a function of phosphorus doping. We find that the SDW transition associated with the Fe moments can be suppressed upon P doping and obtain bulk SC phase transition up to 28 K for $x=0.2$. Further increasing the P content, SC vanishes and Eu^{2+} ordering changes from AF to FM. Our results suggest that SC and FM phases compete with each other. Careful analysis also shows that bulk SC phase co-exists with Eu AF phase, possibly in orthorhombic symmetry. Density functional theory based calculations also witnesses a change in the ordering of the Eu^{2+} moments from AF to FM with increasing phosphorus content. Further analysis also allows us to infer that the lattice effects is more conducive to the onset of SC rather than the phosphorus substitution itself. More microscopic experiments like μSR , low temperature powder diffraction, NMR etc. are currently in progress to confirm the different phases reported here.

The authors would like to thank, C. Geibel, Y. Tokiwa and K. Winzer for discussion and help. We acknowledge financial support by the DFG Research Unit SPP-1458.

¹ N. D. Mathur, F. M. Grosche, S. R. Julian, I. R. Walker, D. M. Freye, R. K. W. Haselwimmer, G. G. Lonzarich, Nature **394**, 39-43 (1998).

² O. Stockert, E. Faulhaber, G. Zwirgagl, N. Stüßer, H.S. Jeevan, M. Deppe, R. Borth, R. Küchler, M. Loewenhaupt,

C. Geibel, and F. Steglich, Phys. Rev. Lett. **92**, 136401 (2004).

³ N. K. Sato, N. Aso, K. Miyake, R. Shiina, P. Thalmeier, G. Varelogiannis, C. Geibel, F. Steglich, P. Fulde, and T. Komatsubara, Nature **410**, 340 (2001).

- ⁴ Y. Kamihara, T. Watanabe, M. Hirano, and H. Hosono, *J. Am. Chem. Soc.* **130**, 3296 (2008).
- ⁵ H. Takahashi, K. Igawa, K. Arii, Y. Kamihara, M. Hirano, and H. Hosono, *Nature*. **453**, 376 (2008).
- ⁶ X. H. Chen, T. Wu, G. Wu, R. H. Liu, H. Chen and D. F. Fang, *Nature*. **453**, 761 (2008).
- ⁷ G.F. Chen, Z. Li, D. Wu, G. Li, W.Z. Hu, J. Dong, P. Zheng, J.L. Luo, and N.L. Wang, *Phys. Rev. Lett.* **100**, 247002 (2008).
- ⁸ M. Rotter, M. Tegel, and D. Johrendt, *Phys. Rev. Lett.* **101**, 107006 (2008).
- ⁹ H. S. Jeevan, Z. Hossain, D. Kasinathan, H. Rosner, C. Geibel, and P. Gegenwart, *Phys. Rev. B* **78**, 092406 (2008).
- ¹⁰ K. Sasmal, B. Lv, B. Lorenz, A. M. Guloy, F. Chen, Y. Y. Xue, and C. W. Chu, *Phys. Rev. Lett.* **101**, 107007 (2008).
- ¹¹ G. Wu, H. Chen, T. Wu, Y. L. Xie, Y. J. Yan, R. H. Liu, X. F. Wang, J. J. Ying, and X. H. Chen, *J. Phys.: Condens. Matter* **20**, 422201 (2008).
- ¹² F. C. Hsu, J. Y. Luo, K. W. Yeh, T. K. Chen, T. W. Huang, Phillip. M. Wu, Y. C. Lee, Y. L. Huang, Y. Y. Chu, D. C. Yan, and M. K. Wu, *Proc. Natl. Acad. Sci. USA* **105**, 14262(2008).
- ¹³ H. S. Jeevan, Z. Hossain, Deepa Kasinathan, H. Rosner, C. Geibel, and P. Gegenwart, *Phys. Rev. B* **78**, 052502 (2008).
- ¹⁴ Y. Qi , Gao Z, Wang L, Wang D, Zhang X and Ma Y 2008 *New J. Phys.* **10** 123003
- ¹⁵ Z. Ren, Q. Tao, S. Jiang, C. Feng, C. Wang, J. Dai, G. Cao, and Z. Xu, *Phys. Rev. Lett.* **102**, 137002 (2009).
- ¹⁶ C. F. Miclea, M. Nicklas, H. S. Jeevan, D. Kasinathan, Z. Hossain, H. Rosner, P. Gegenwart, C. Geibel, and F. Steglich, *Phys. Rev. B* **79**, 212509 (2009).
- ¹⁷ C. Feng, Z. Ren, S. Xu, Z. Xu, G. Cao, I. Nowik, I. Felner, K. Matsubayashi, and Y. Uwatoko, *Phys. Rev. B* **82**, 094426 (2010).
- ¹⁸ S. Jiang, H. Xing, G. Xuan, C. Wang, Z. Ren, C. Feng, J. Dai, Z. Xu, G. Cao, *J. Phys.: Condens. Matter*, **21**, 382203 (2009)
- ¹⁹ Z. Ren, X. Lin, Q. Tao, S. Jiang, Z. Zhu, C. Wang, G. Cao, and Z. Xu, *Rev. B* **79**, 094426 (2009).
- ²⁰ S. Nandi, M. G. Kim, A. Kreyssig, R. M. Fernandes, D. K. Pratt, A. Thaler, N. Ni, S. L. Budko, P. C. Canfield, J. Schmalian, R. J. McQueeney, and A. I. Goldman, *Phys. Rev. Lett.* **104**, 057006 (2010).
- ²¹ T. Terashima, M. Kimata, H. Satsukawa, A. Harada, K. Hazama, S. Uji, H. S. Suzuki, T. Matsumoto, and K. Murata, *J. Phys. Soc. Jpn.* **78**, 083701 (2009)
- ²² S. R. Saha, N. P. Butch, K. Kirshenbaum, and Johnpierre Paglione, *Phys. Rev. B* **79**, 224519 (2009)
- ²³ L. J. Li, Y. K. Luo, Q. B. Wang, H. Chen, Z. Ren, Q. Tao, Y. K. Li, X. Lin, M. He, Z. W. Zhu, G. H. Cao, and Z. A. Xu, *New J. Phys.* **11**, 025008 (2009)
- ²⁴ N. Kumar, S. Chi, Y. Chen, K. G. Rana, A. K. Nigam, A. Thamizhavel, W. Ratcliff II, S. K. Dhar, and J. W. Lynn, *Phys. Rev. B* **80**, 144524 (2009)
- ²⁵ S. Thirupathaiah, E.D.L. Rienks, H.S. Jeevan, R. Ovsyannikov, E. Slooten, J. Kaas, E. van Heumen, S. de Jong, H.A. Duerr, K. Siemensmeyer, R. Follath, P. Gegenwart, M.S. Golden, J. Fink, arXiv:1007.5205
- ²⁶ L. Rettig, R. Cortes, S. Thirupathaiah, P. Gegenwart, H.S. Jeevan, T. Wolf, U. Bovensiepen, M. Wolf, H.A. Drr, J. Fink, arXiv:1008.1561
- ²⁷ D. Wu, G. Chanda, H. S. Jeevan, P. Gegenwart, M. Dressel, arXiv:1011.1207
- ²⁸ K. Koepf, and H. Eschrig, *Phys. Rev. B* **59**, 1743 (1999).
- ²⁹ J. P. Perdew and Y. Wang, *Phys. Rev. B* **45**, 13244 (1992).
- ³⁰ M. T. Czyżyk and G. A. Sawatzky, *Phys. Rev. B* **49**, 14211 (1994).
- ³¹ T. Terashima, N. Kurita, A. Kikkawa, H. S. Suzuki, T. Matsumoto, K. Murata, and S. Uji, *J. Phys. Soc. Japan* **79**, 103706 (2010)
- ³² Y. Xiao, Y. Su, W. Schmidt, K. Schmalzl, C. M. N. Kumar, S. Price, T. Chatterji, R. Mittal, L. J. Chang, S. Nandi, S. K. Dhar, A. Tamizhavel, and T. Brueckel, *Phys. Rev. B* **81**, 220406 (2010).
- ³³ E. Mörsen, B. D. Mosel, W. Müller Warmuth, M. Reehuis, and W. Jeitschko, *J. Phys. Chem. Solids* **49**, 785 (1988).
- ³⁴ L. Sun, J. Guo, G. Chen, X. Chen, X. Dong, W. Lu, C. Zhang, Z. Jiang, Y. Zhou, S. Zhang, Y. Huang, Q. Wu, X. Dai, Y. Li, J. Liu, and Z. Zhao, *Phys. Rev. B* **82**, 134509 (2010).